



**HAL**  
open science

# Search for the Higgs boson in fermionic channels using ATLAS detector

Kazuya Mochizuki

► **To cite this version:**

Kazuya Mochizuki. Search for the Higgs boson in fermionic channels using ATLAS detector. Workshop on Discovery Physics at the LHC (Kruger 2014), Dec 2014, Mpumalanga, South Africa. pp.012020, 10.1088/1742-6596/623/1/012020 . hal-01231398

**HAL Id: hal-01231398**

**<https://amu.hal.science/hal-01231398>**

Submitted on 20 Nov 2015

**HAL** is a multi-disciplinary open access archive for the deposit and dissemination of scientific research documents, whether they are published or not. The documents may come from teaching and research institutions in France or abroad, or from public or private research centers.

L'archive ouverte pluridisciplinaire **HAL**, est destinée au dépôt et à la diffusion de documents scientifiques de niveau recherche, publiés ou non, émanant des établissements d'enseignement et de recherche français ou étrangers, des laboratoires publics ou privés.

## Search for the Higgs boson in fermionic channels using ATLAS detector

This content has been downloaded from IOPscience. Please scroll down to see the full text.

2015 J. Phys.: Conf. Ser. 623 012020

(<http://iopscience.iop.org/1742-6596/623/1/012020>)

View [the table of contents for this issue](#), or go to the [journal homepage](#) for more

Download details:

IP Address: 147.94.212.92

This content was downloaded on 20/11/2015 at 09:51

Please note that [terms and conditions apply](#).

# Search for the Higgs boson in fermionic channels using ATLAS detector

**Kazuya Mochizuki, on behalf of the ATLAS collaboration**

CPPM, Aix-Marseille Université, CNRS/IN2P3, Marseille, France

E-mail: [kazuya.mochizuki@cern.ch](mailto:kazuya.mochizuki@cern.ch)

**Abstract.** The property measurements of the recently discovered boson at a mass around 125 GeV confirm that it is compatible with the Higgs boson predicted by the Standard Model. Since the discovery and the first property measurements were performed using the bosonic decay channels, it is particularly important to observe and measure the Higgs boson using the fermionic decay channels. We present a review of the searches for the Higgs boson decaying to a pair of  $\tau$ -leptons, muons, and  $b$ -quarks with the ATLAS experiment using LHC Run 1 full dataset.

## 1. Introduction

In July 2012, the ATLAS [1] and CMS [2] experiments announced the discovery of a new boson at a mass of around 125 GeV [3, 4]. The compatibility of this boson with the Standard Model (SM) prediction was confirmed by measuring properties such as spin, parity, and signal strength at the measured mass using bosonic decay channels, namely  $H \rightarrow \gamma\gamma$ ,  $ZZ^*$ , and  $WW^*$ , thanks to their clean signatures in the final state. In order to fully determine whether this is the SM Higgs boson, it is crucial to observe and measure the Higgs boson using also fermionic channels. In this proceedings article, we report the current status of these searches with the ATLAS experiment.  $H \rightarrow \tau\tau$ ,  $\mu\mu$ , and  $bb$  searches are reviewed in section 2, 3, and 4, respectively. These searches are performed using the full ATLAS dataset recorded in LHC Run 1. The integrated luminosity collected in the year 2011 (2012) is 4.6 (20.3)  $\text{fb}^{-1}$  at a center-of-mass energy of 7 (8) TeV\*.

## 2. $H \rightarrow \tau\tau$

In this section, the search for  $H \rightarrow \tau\tau$  decays is summarized [5]. The branching ratio (BR) of  $H \rightarrow \tau\tau$  is 6.3% at  $m_H = 125$  GeV, due to the relatively high mass of the  $\tau$ -lepton ( $m_\tau = 1.78$  GeV). Because of the presence of undetected neutrinos produced by the  $\tau$ -decays, the invariant mass of the visible decay components is smaller than the actual  $\tau\tau$  invariant mass ( $m_{\tau\tau}$ ). To reconstruct  $m_{\tau\tau}$  correctly, the missing mass calculator (MMC) is employed. The MMC scans through the  $\tau$ -lepton decay probability density functions using the reconstructed  $E_T^{\text{miss}}$  and visible  $\tau$ -lepton mass and then calculates the most likely  $\tau\tau$  invariant mass ( $m_{\tau\tau}^{\text{MMC}}$ ).

### 2.1. Event selection and categorization

Since  $\tau$  leptons decay either leptonically or hadronically, the analysis is split into three channels, which are  $\tau_{\text{lep}}\tau_{\text{lep}}$ ,  $\tau_{\text{lep}}\tau_{\text{had}}$ , and  $\tau_{\text{had}}\tau_{\text{had}}$  where  $\tau_{\text{lep}}$  is a leptonic  $\tau$ -decay object ( $\tau \rightarrow \nu_\tau \nu_\ell \ell$  with  $\ell = e, \mu$ ) and  $\tau_{\text{had}}$  is a hadronic  $\tau$ -decay object ( $\tau \rightarrow \nu_\tau$  hadrons).

\* The 7 TeV dataset in the  $H \rightarrow bb$  search corresponds to an integrated luminosity of 4.7  $\text{fb}^{-1}$ .



The BRs for  $\tau_{\text{lep}}\tau_{\text{lep}}$ ,  $\tau_{\text{lep}}\tau_{\text{had}}$ , and  $\tau_{\text{had}}\tau_{\text{had}}$  are 12.4%, 45.6%, and 42%, respectively. Across all three channels, the dominant and irreducible background is  $(Z \rightarrow \tau\tau)+\text{jets}$ , which is estimated with  $\tau$ -embedding techniques\*. Other background processes, depending on the channels and categories, are top quark production, diboson production, and fakes of leptons or hadronic  $\tau$ -decays mainly caused by  $W+\text{jets}$  or multijet events (see Fig 1).

Events are primarily selected by dilepton, single lepton, and di-hadronic tau triggers for  $\tau_{\text{lep}}\tau_{\text{lep}}$ ,  $\tau_{\text{lep}}\tau_{\text{had}}$ , and  $\tau_{\text{had}}\tau_{\text{had}}$  channels, respectively. Since the charge information of the  $\tau$ -lepton is always inherited by its decay product(s), the analysis requires opposite charges for the decay objects of  $\tau$ -pairs. For the channels involving  $\tau_{\text{lep}}$ , isolation requirements on electrons or muons are applied, which are dependent on the center-of-mass energy and pileup conditions. To suppress the  $t\bar{t}$  background contributions, events with  $b$ -tagged jets † with  $|\eta^{\text{jet}}| < 2.5$  are rejected in the  $\tau_{\text{lep}}\tau_{\text{lep}}$  and  $\tau_{\text{had}}\tau_{\text{had}}$  channels.

**$\tau_{\text{lep}}\tau_{\text{lep}}$ :** Events with exactly two isolated leptons are selected. No additional  $\tau_{\text{had}}$  or  $\tau_{\text{lep}}$  candidates are allowed. The lepton isolation requirement for both leptons reduces the multijet background contribution in this channel.

**$\tau_{\text{lep}}\tau_{\text{had}}$ :** Events with exactly one isolated lepton and exactly one  $\tau_{\text{had}}$  candidate are selected. To reduce the  $W+\text{jets}$  background, a selection on the transverse mass is applied,  $m_{\text{T}}(\ell, E_{\text{T}}^{\text{miss}}) < 70$  GeV.

**$\tau_{\text{had}}\tau_{\text{had}}$ :** In the  $\tau_{\text{had}}\tau_{\text{had}}$  channel,  $\tau_{\text{had}}$  isolation is required. One isolated medium and one isolated tight  $\tau_{\text{had}}$  candidates are required in an event with  $E_{\text{T}}^{\text{miss}} > 20$  GeV. Events with electron or muon candidates are rejected. To suppress the main multijet background in this channel, selections are applied on angular separation variables such as  $\Delta R(\tau_{\text{had}}, \tau_{\text{had}})$  and  $\Delta\eta(\tau_{\text{had}}, \tau_{\text{had}})$ .

The search is targeted at two production processes of the Higgs boson, which are vector boson fusion (VBF), and gluon fusion ( $ggH$ ) which is targeted by the Boosted category, where the Higgs boson has  $p_{\text{T}}^H > 100$  GeV. Events are first required to pass the pre-selections before the selections of those VBF and Boosted categories. The VBF category provides the best sensitivity because of the very discriminative event topology in which two high  $p_{\text{T}}$  jets have a large pseudo-rapidity separation ( $\Delta\eta(j_1, j_2)$ , see Fig 1). Therefore, events failing to be classified in the VBF category are considered as candidates for the Boosted category.

## 2.2. Multivariate analysis and global likelihood fit

To improve the separation between the signal and background, various kinematic properties are combined together with  $m_{\tau\tau}^{\text{MMC}}$  by boosted decision trees (BDT). In addition to the simulated samples, some data driven samples are also used for the backgrounds. The BDTs are trained in six categories, which consist of  $\tau_{\text{lep}}\tau_{\text{lep}}$ ,  $\tau_{\text{lep}}\tau_{\text{had}}$ , and  $\tau_{\text{had}}\tau_{\text{had}}$  channels in each of the Boosted and VBF categories. The number of input variables used in these BDTs varies from 5 to 9 depending on the category. These variables describe kinematic properties of the  $\tau\tau$  system and jet properties especially in the VBF category. Examples of these input variables are shown in Fig 1. Figure 2 shows the BDT output distributions in the most sensitive channel,  $\tau_{\text{lep}}\tau_{\text{had}}$ , in the VBF and Boosted categories separately.

The signal strength  $\mu$  is extracted from a simultaneous maximum-likelihood fit to the BDT discriminants in the six categories. To constrain the background contributions, this fit is performed also on the event yields in dedicated control regions (CR) for the specific backgrounds in each category. For the  $\tau_{\text{lep}}\tau_{\text{lep}}$  and  $\tau_{\text{lep}}\tau_{\text{had}}$  channels,  $Z \rightarrow \tau\tau$ -enriched,  $Z \rightarrow \ell\ell$ -enriched, fake-enriched, and top CRs are defined. A ‘rest’ category is defined for the  $\tau_{\text{had}}\tau_{\text{had}}$  channel, where the events pass the pre-selection but not the VBF or Boosted selection. In the  $\tau_{\text{had}}\tau_{\text{had}}$

\* The shape of the  $(Z \rightarrow \tau\tau)+\text{jets}$  is estimated from  $(Z \rightarrow \mu\mu)+\text{jets}$  in data, where muons are replaced with simulated  $\tau$ -decays.

† Jets identified as originating from  $b$ -quark fragmentation by MV1  $b$ -tagging algorithm [6, 7]. The operating point used in this search provides 60–70% efficiency for  $b$ -jets in simulated  $t\bar{t}$  events.

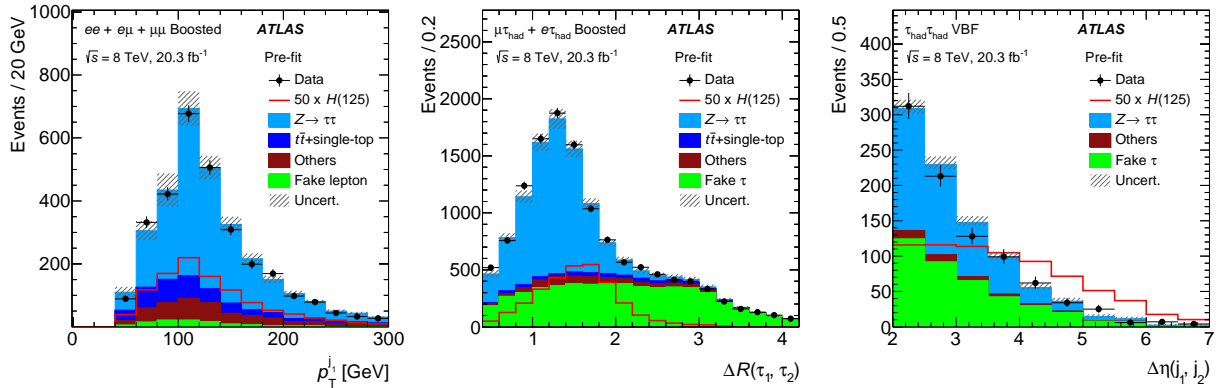


**Figure 1.** Distributions of important BDT input variables for data collected at a center-of-mass energy of 8 TeV. Leading jet  $p_T$  in Boosted  $\tau_{lep}\tau_{lep}$  category (left),  $\Delta R(\tau_{lep}, \tau_{had})$  in Boosted  $\tau_{lep}\tau_{had}$  category (middle) and  $\Delta\eta(j_1, j_2)$  in VBF  $\tau_{had}\tau_{had}$  category (right). The contributions from the SM Higgs boson with  $m_H = 125$  GeV are multiplied by a factor of 50 and superimposed. The error band includes statistical and pre-fit systematic uncertainties [5].

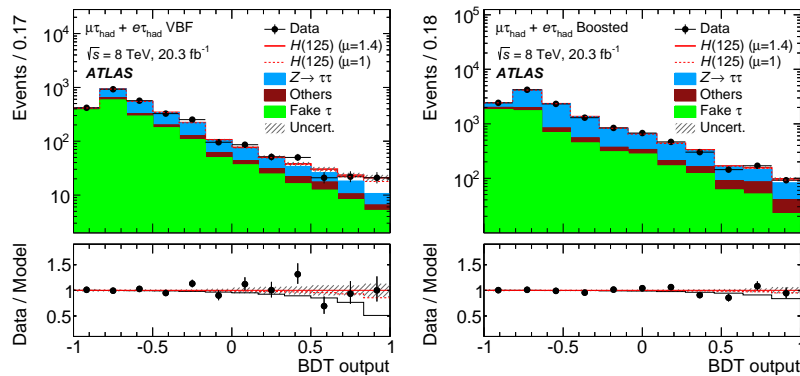


**Figure 2.** Distributions of the BDT discriminant for data taken at center-of-mass energy of 8 TeV in the signal regions of the VBF (left) and Boosted (right) categories for the  $\tau_{lep}\tau_{had}$  channel. The Higgs boson signal ( $m_H = 125$  GeV) is shown stacked with a signal strength of  $\mu = 1.0$  (dashed red line) and  $\mu = 1.4$  (solid red line). The size of the statistical and systematic normalization uncertainties is indicated by the hashed band. The data ratios to the models (background plus Higgs boson contributions with  $\mu = 1.4$ ) are shown in the lower panels. The dashed red and the solid black lines represent the changes in the model when  $\mu = 1.0$  or background-only are assumed respectively [5].

channel,  $\tau\tau$  invariant mass side-bands ( $m_{\tau\tau}^{MMC} < 110$  GeV or  $m_{\tau\tau}^{MMC} > 150$  GeV) are also used to constrain the backgrounds.

### 2.3. Results

Figure 3 shows the combined results from all the analysis categories. An excess over the SM background prediction is observed. The extracted signal strength with the global maximum-likelihood fit is  $\mu = 1.43^{+0.27}_{-0.26}$  (stat.) $^{+0.32}_{-0.25}$  (syst.)  $\pm 0.09$  (theo.) for  $m_H = 125.36$  GeV. The dominant sources of systematic uncertainties are energy scales of the jets and  $\tau_{had}$ , identification of  $\tau_{had}$ , and background normalization. The probability  $p_0$  of obtaining a result at least as signal-like as observed in data without signal presence is calculated. For  $m_H = 125.36$  GeV, the observed  $p_0$  value is  $2.7 \times 10^{-6}$ , which corresponds to a  $4.5\sigma$  deviation from the background only hypothesis,

while  $3.4\sigma$  deviation is expected. This provides evidence for  $H \rightarrow \tau\tau$  at  $m_H = 125.36$  GeV.

The two dimensional likelihood contours of the signal strength parameters for production modes of VBF and  $ggH$  are shown in Fig 3. The results are compatible with the SM predictions within  $1\sigma$ .

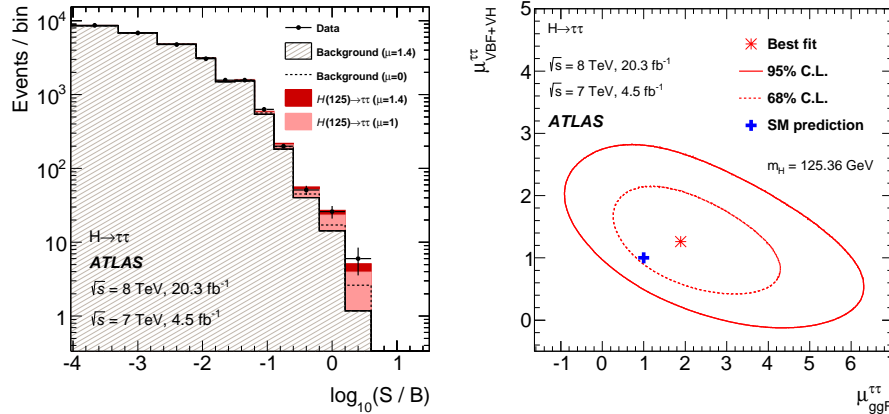


**Figure 3.** Combined results from  $\tau_{\text{lep}}\tau_{\text{lep}}$ ,  $\tau_{\text{lep}}\tau_{\text{had}}$ , and  $\tau_{\text{had}}\tau_{\text{had}}$  channels in VBF and Boosted categories. The left plot shows event yields as a function of  $\log_{10}(S/B)$ , where  $S$  (signal yield) and  $B$  (background yield) are taken from the BDT output bin of each event, assuming  $\mu = 1.4$ . The predicted background is obtained from the global fit (with  $\mu = 1.4$ ) and signal yields are shown for  $m_H = 125$  GeV, at  $\mu = 1$  and  $\mu = 1.4$  (best-fit value). The background only distribution (dashed line) is obtained from the global fit, but fixing  $\mu = 0$ . The right plot shows the likelihood contours for the combination of all channels in the  $(\mu_{ggF}^{\tau\tau}, \mu_{VBF+VH}^{\tau\tau})$  plane. The 68% (95%) CL contour is shown as dashed (solid) line for  $m_H = 125.36$  GeV. The SM expectation is shown by a filled plus symbol. The best fit to data is shown for the case when both the  $\mu_{ggF}^{\tau\tau}$  and  $\mu_{VBF+VH}^{\tau\tau}$  are unconstrained [5].

### 3. $H \rightarrow \mu\mu$

This section reviews the search for  $H \rightarrow \mu\mu$  decays [8]. This decay channel is particularly important to measure the Higgs-lepton second generation couplings. In the SM, the BR of  $H \rightarrow \mu\mu$  is 0.02% at  $m_H = 125$  GeV due to the light muon mass. It suffers from the overwhelming and irreducible Drell-Yan background. The analysis focuses on the search for a narrow resonance, exploiting the very high resolution of the  $\mu\mu$  invariant mass ( $m_{\mu\mu}$ ). The dominant background in this search is  $Z^*/\gamma \rightarrow \mu\mu$  production, followed by smaller backgrounds from single and pair production of the top quarks and diboson processes.

#### 3.1. Event selection, categorization and modeling

The trigger used for this search is a combination of single muon and dimuon triggers. The events are required to have two oppositely charged isolated muons with  $p_T > 15$  GeV, where at least one muon must have  $p_T > 25$  GeV. All muon candidates are required to be within  $|\eta| < 2.5$ . To suppress the  $t\bar{t}$  and diboson background processes,  $E_T^{\text{miss}} < 80$  GeV is required.

After the pre-selection described above, the categorization is performed for VBF and  $ggH$  to maximize the sensitivity. As for the  $H \rightarrow \tau\tau$  search presented in Sec. 2, events are first checked for the VBF category, then for  $ggH$  category. In the VBF category, at least two jets are required with  $\Delta\eta(j_1, j_2) > 3$  and  $m(j_1, j_2) > 500$  GeV. In the  $ggH$  category, the events are further divided into six categories depending on  $|\eta^\mu|$  and transverse momentum of the Higgs boson candidate ( $p_T^{\mu\mu}$ ). The event is categorized as ‘central’ category if both muons satisfy

$|\eta^\mu| < 1$  and as ‘non-central’ otherwise. These central and non-central categories are split into three categories based on  $p_T^{\mu\mu}$  with boundaries at 15 and 50 GeV. A CR is defined for  $W$ +jets background, where one of the jets is misidentified as a muon, by requiring same-sign charges for the muon candidates.

The Higgs signal shape is fit to simulated data with the sum of Crystal Ball and Gaussian functions. Background modeling for the  $ggH$  category uses a Breit-Wigner (BW) function convoluted with a Gaussian function while the product of a BW function and an exponential function is taken for the VBF category. To derive the results, a binned maximum likelihood fit is done to the  $m_{\mu\mu}$  distribution in the range 110-160 GeV simultaneously in all seven categories with separate distributions in 7 and 8 TeV data. Examples of the fit in 8 TeV data are shown in Fig 4.

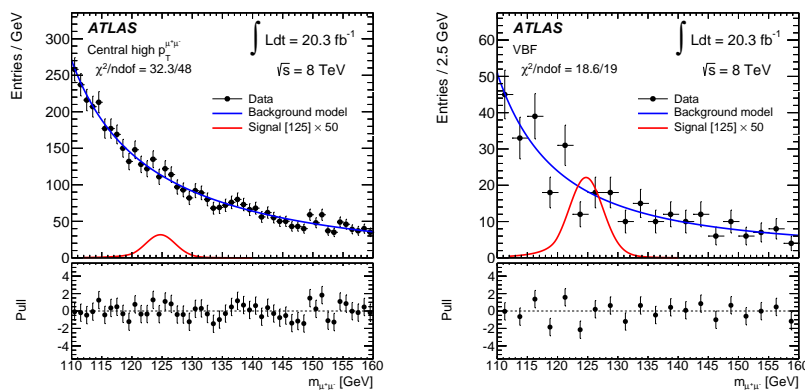


**Figure 4.** The background model fits to the  $m_{\mu\mu}$  distribution for 8 TeV data for the central high  $p_T^{\mu\mu}$  category (left) and VBF category (right). The statistical uncertainties are given for the data points. The expected signal is shown for  $m_H = 125$  GeV, scaled by a factor of 50 [8].

### 3.2. Results

The observed data are consistent with the expected backgrounds and no excess is observed. For  $m_H = 125.5$  GeV, the observed (expected) limit on the signal strength at 95% CL limit is 7.0 (7.2) times the SM prediction. Under the assumption of  $m_H = 125.5$  GeV with the SM production cross section, the 95% CL upper limit on the  $H \rightarrow \mu\mu$  BR is  $1.5 \times 10^{-3}$ . The search is limited by the statistics.

## 4. $H \rightarrow bb$

This section presents the search for  $H \rightarrow bb$  decays [9].  $H \rightarrow bb$  has the largest BR of 58% at  $m_H = 125$  GeV. In this decay channel, VBF and  $ggH$  production modes are overwhelmed by  $b$ -quark pair production at the LHC. Therefore, the analysis focuses on the  $VH$  production ( $VH \rightarrow Vbb$ ) mode where the associated vector boson ( $V$ ) provides a clear tag for the search.

### 4.1. Event selection and categorization

According to the number of leptons in the final state the search is split into three channels of 0-lepton, 1-lepton, and 2-lepton, targeting  $ZH \rightarrow \nu\nu bb$ ,  $WH \rightarrow \ell\nu bb$ , and  $ZH \rightarrow \ell\ell bb$  processes ( $\ell = e, \mu$ ), respectively. A further categorization is performed in this search based on the  $p_T$  of the vector boson, defining low and high  $p_T^V$  intervals with a boundary at 120 GeV. The dominant background for this search is  $V$ + jets events, especially the  $V$ + heavy flavor jets which remain after  $b$ -tagging requirements. Diboson ( $VZ$ ) production generates almost the same event

signatures as the  $VH$  signal. The  $VZ$  production has slightly higher cross-section than  $VH$  signal, however smaller than the other backgrounds. Therefore,  $VZ$  production is used to validate the search results by measuring the signal strength  $\mu_{VZ}$ . The other backgrounds are single and pair production of top quarks, and multijet events. Across the three channels, events are required to have two  $b$ -tagged jets with  $p_T > 20$  GeV, with at least one jet with  $p_T > 45$  GeV. Events with forward jets ( $|\eta^{\text{jet}}| > 2.5$ ) are discarded for  $t\bar{t}$  rejection. Events with a third (non  $b$ -tagged) jet are allowed and form a separate category, called the 3-jet bin. This analysis employs MV1c  $b$ -tagging algorithm which is a variant of MV1 tagging algorithm with improved  $c$ -jet rejection and a modest cost in light flavor jet rejection. Depending on the tightness of the operating point of the MV1c, three categories are defined which are 2 tight tags (TT), 2 medium tags (MM), and 2 light tags (LL).

**0-lepton:** Events in this channel are selected with an  $E_T^{\text{miss}}$  trigger which is 100%, 97%, and 80% efficient for  $E_T^{\text{miss}} > 160$ ,  $E_T^{\text{miss}} > 120$  and  $E_T^{\text{miss}} > 100$  GeV. This channel requires very large  $E_T^{\text{miss}}$  in the event,  $E_T^{\text{miss}} > 100$  GeV, caused by a high  $p_T$   $Z$  boson decaying to a pair of neutrinos. Many kinematic selections are applied to suppress the multijet and top quark backgrounds. In the 3-jet bin, events with  $p_T^V < 120$  are not used.

**1-lepton:** The main trigger for this channel is single lepton (single electron or single muon) trigger. To recover the events missed by the muon trigger, the  $E_T^{\text{miss}}$  trigger is also used in the high  $p_T^V$  muon channel. The events are required to have exactly one isolated lepton (electron or muon) with  $p_T > 20$  GeV, with large  $H_{T^*}$  or  $E_T^{\text{miss}}$  in the low and high  $p_T^V$  intervals, respectively. The low  $p_T^V$  electron channel is excluded from the analysis.

**2-lepton:** Events in this channel are selected with a combination of single lepton and dilepton (dielectron or dimuon) triggers. This channel profits from the very clean signature provided by the leptonic decay of the  $Z$  boson. Events must have two isolated same flavor leptons with opposite electric charges. The events are required to have dilepton invariant mass in the range 83–99 GeV.

#### 4.2. Multivariate analysis and fit model

Similarly to the  $H \rightarrow \tau\tau$  search, BDTs are constructed for 10 categories of signal regions in 0-, 1-, and 2-lepton channels, 2 and 3-jet bins, and low and high  $p_T^V$  categories†. Depending on the category, additional kinematic properties and  $b$ -jet properties are used to build BDTs together with the most important variable  $m_{bb}$ . Figure 5 shows the BDT output distributions in the most sensitive regions of the search.

Multijet backgrounds are estimated using data, since they cannot be estimated with simulated events. In the 0-lepton channel, multijet background is estimated using the so-called ‘‘ABCD method’’ using  $\min[\Delta\phi(E_T^{\text{miss}}, \text{jet})]$  and  $\Delta\phi(E_T^{\text{miss}}, p_T^{\text{miss}})$ . In the 1-lepton channel, the multijet fit is performed on the  $E_T^{\text{miss}}$  distribution using a CR defined by loosened lepton isolation requirements. In the 2-lepton channel, multijet background is also estimated with the fit to  $m_{\ell\ell}$  using a CR defined in similar way to the 1-lepton channel by loosened lepton isolation and identification criteria.

The signal strength  $\mu$  is extracted by a maximum-likelihood fit to the BDT distributions in the 24 2-tag signal regions defined by three lepton channels, up to two  $p_T^V$  intervals, the two number of jet bins, and  $b$ -tagging categories. In the 0 and 2-lepton channels, the TT and MM  $b$ -tagging categories are merged while they are kept separated in the 1-lepton channel. In the 1-lepton channel, the 2-tag signal regions in the 3-jet bin effectively play the role of CRs because  $t\bar{t}$  background dominates these regions. The  $b$ -tagging discriminant, MV1c, is used in the global fit in the 11 1-tag CRs for three lepton channels, two jet bins, and two  $p_T^V$  intervals.

\* Scalar sum of  $E_T^{\text{miss}}$  and  $p_T$  of the lepton and leading two jets.

† In low  $p_T^V$  0-lepton channel, the variable used in the global fit is  $m_{bb}$  instead of the BDT discriminant.

This particularly improves the normalization of the  $V$  + light flavor jets backgrounds.

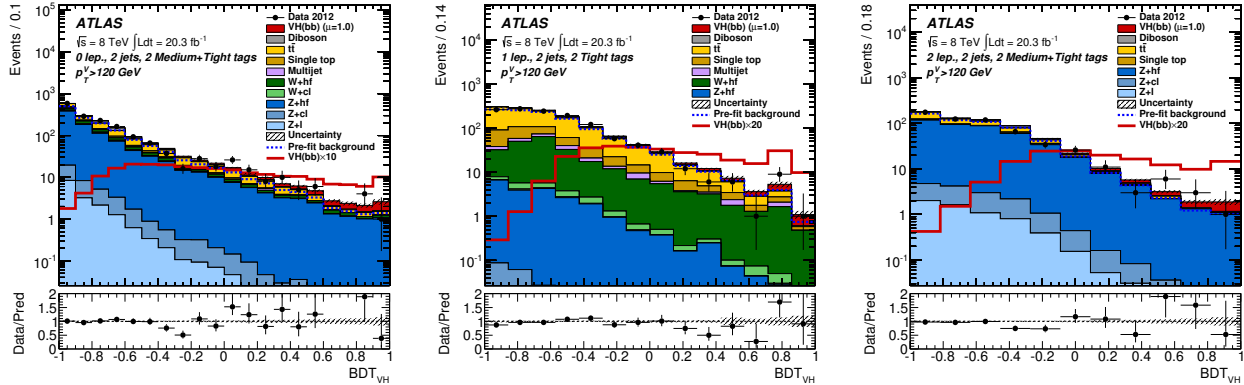


**Figure 5.** The BDT discriminant distributions in 2-jet high  $p_T^V$  categories in MM+TT category 0-lepton channel (left), TT category 1-lepton channel (middle), and MM+TT 2-lepton channel (right). The background contributions after the global fit of the MVA are shown as filled histograms along with the data points. The Higgs boson signal is shown as filled histogram on top of the fitted backgrounds as predicted by the SM ( $\mu = 1$ ), and unstacked open histogram, multiplied by a factor 20. The dashed histogram shows the pre-fit total background. The hatched band shows the statistical and systematic uncertainties. The data ratio to the signal + fitted background is shown in the lower panel [9].

#### 4.3. Results

Figure 6 shows the combined results from all the analysis categories. An excess is observed (expected) at the  $1.4\sigma$  ( $2.6\sigma$ ) level over the background-only hypothesis. The measured signal strength is  $\mu_{VH} = 0.52 \pm 0.32(\text{stat.}) \pm 0.24(\text{syst.})$  for  $m_H = 125.36$  GeV. The dominant sources of systematic uncertainties are shape and normalization modelings of the  $V$  + heavy flavor jets background.

Two cross-checks are performed using the  $VZ$  and dijet mass analyses in 8 TeV data. For the cross-check with  $VZ$ , a BDT is trained for  $VZ$  signal events instead of  $VH$  signals. The measured signal strength is  $\mu_{VZ} = 0.77 \pm 0.10(\text{stat.}) \pm 0.15(\text{syst.})$ , which is consistent with the SM. The cross-check with the dijet mass analysis is done by performing a fit to the  $m_{bb}$  distribution rather than to the BDT discriminant. In this cross-check, the selections are tighter, with finer  $p_T^V$  intervals (see Fig 6). The measured signal strength of the Higgs boson signal is  $\mu_{VH} = 1.23 \pm 0.44(\text{stat.}) \pm 0.41(\text{syst.})$ . The observed (expected) significance of an excess over the background-only hypothesis is  $2.2\sigma$  ( $1.9\sigma$ ) in the dijet mass cross-check.

Figure 7 shows the signal strength measured separately in 7 and 8 TeV data as well as in the three lepton channels for the combined sample.

## 5. Summary

Higgs boson searches in decay channels to  $\tau\tau$ ,  $\mu\mu$  and  $bb$ , performed in the ATLAS experiment, are presented. Direct evidence of  $H \rightarrow \tau\tau$  is observed. The  $H \rightarrow \mu\mu$  search is not sensitive yet because of the limited data statistics. However, the result confirms non-universal couplings of  $H \rightarrow \ell\ell$  as predicted by the SM. An excess with  $1.4\sigma$  significance is observed in the  $VH \rightarrow Vbb$  search. Overall, all the results are compatible with the SM predictions. The LHC Run 2 will provide data with an increased center-of-mass energy of 13 TeV in 2015 and at higher luminosity, which will allow for more precise studies of the Higgs boson properties in fermionic decay channels.

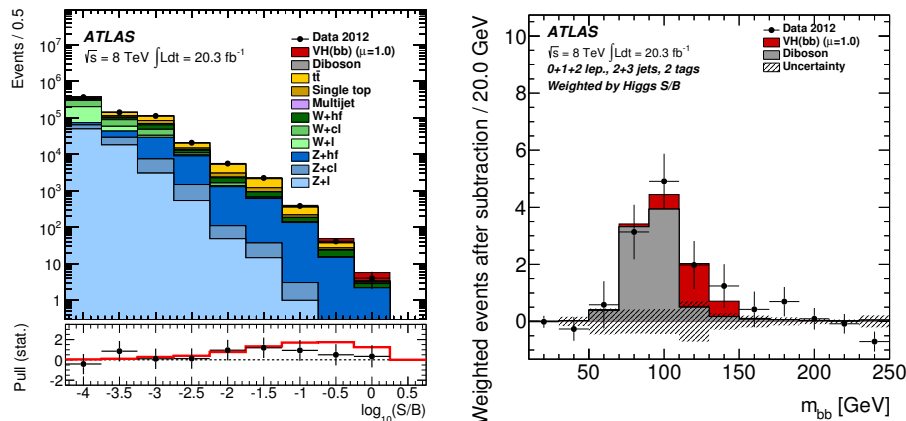


**Figure 6.** The left plot shows event yields as a function of  $\log(S/B)$  for data, background and Higgs boson signal with  $m_H = 125$  GeV for the 8 TeV data in 0-, 1- and 2-lepton channels of the  $H \rightarrow bb$  analysis. The Higgs boson signal contribution is stacked on top of background with  $\mu = 1.0$ . The pull of data with respect to the background-only prediction is also shown with statistical uncertainties only. The red line shows the pull of the background + signal ( $\mu = 1.0$ ) with respect to the background-only prediction. The right plot shows the  $m_{bb}$  distribution after subtraction of all the backgrounds except the  $VZ$  processes, for the dijet mass cross-check performed for the 8 TeV data. The contributions from all lepton channels,  $p_T^V$  intervals, number of jet bins, and 2-tag  $b$ -tagging categories are summed with weights defined by their respective S/B ratio after the global fit. The Higgs boson signal is stacked over the  $VZ$  contribution with  $\mu = 1.0$ . The hatched band shows the size of the statistical and systematic uncertainty on the fitted background [9].

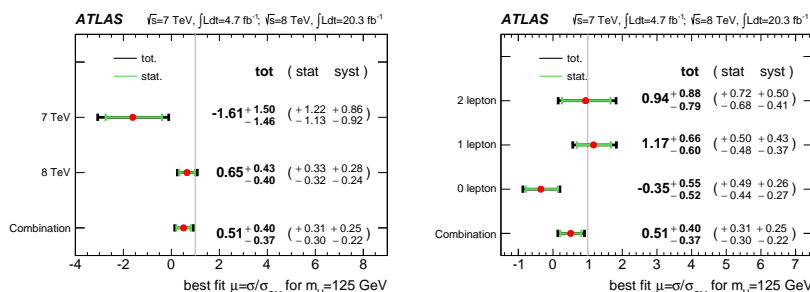


**Figure 7.** The signal strength measured separately in 7 and 8 TeV data (left) and in the 0-, 1-, and 2-lepton channels in 7 and 8 TeV data (right) for  $m_H = 125$  GeV. The individual  $\mu$  values for the three lepton channels are obtained from a simultaneous fit with the signal strength for each lepton channel floating independently [9].

## References

- [1] ATLAS Collaboration, JINST **3** (2008) S08003.
- [2] CMS Collaboration, JINST **3** (2008) S08004.
- [3] ATLAS Collaboration, Phys.Lett. **B716** (2012) 1–29, arXiv:1207.7214 [hep-ex].
- [4] CMS Collaboration, Phys.Lett. **B716** (2012) 30–61, arXiv:1207.7235 [hep-ex].
- [5] ATLAS Collaboration, CERN-PH-EP-2014-262 (2015), arXiv:1501.04943 [hep-ex].
- [6] ATLAS Collaboration, ATLAS-CONF-2014-004 (2014). <http://cds.cern.ch/record/1664335>.
- [7] ATLAS Collaboration, ATLAS-CONF-2014-046 (2014). <http://cds.cern.ch/record/1741020>.
- [8] ATLAS Collaboration, Phys.Lett. **B738** (2014) 68–86, arXiv:1406.7663 [hep-ex].
- [9] ATLAS Collaboration, JHEP **1501** (2015) 069, arXiv:1409.6212 [hep-ex].